Synthesis, characterization and crystal structures of a series of tetraosmium carbonyl clusters containing bidentate phosphine ligands

Ya-Yin Choi, Wing-Tak Wong *

Department of Chemistry, The University of Hong Kong, Pokfulam Road, Hong Kong, Hong Kong

Received 22 March 1997; revised 10 May 1997; accepted 10 May 1997

Abstract

Reactions of the activated tetraosmium hydrido cluster 1 with a series of bidentate phosphine ligands $PPh_2(CH_2)_nPPh_2$ ($n = 1$, dppm; $n = 3$, dppp), $PPh_2(CH)_2PPh_2$, (dppee) and $(PPh_2C_5H_4)_2Fe$, (dppf) gave several novel tetraosmium clusters $[Os_4(\mu\text{-H})_4(CO)_{10}(\mu\text{-dppm})]$ 2, $[Os_4(\mu\text{-H})_4(CO)_{10}(\mu\text{-dppee})]$ 3a, $[Os_4(\mu\text{-H})_4(CO)_{10}(\eta^2\text{-dppee})]$ 3b $[Os_4(\mu\text{-H})_4(CO)_{10}(\mu\text{-dppp})]$ 4 and $[Os_4(\mu\text{-H})_4(CO)_{10}(\mu\text{-dppf})]$ 5 in moderate to good yields.

All the complexes were fully characterized by both spectroscopic and crystallographic methods. Each of the structures of 2, 3a, 4 and 5 contains a tetraosmium metal core with a bridging diphosphine ligand. Compound 3a and 3b are geometrical isomers and they differ in the bonding modes of the diphosphine ligand dppee exhibits. A chelating dppee ligand bonded to a single osmium atom is observed in complex 3b. © 1997 Elsevier Science S.A.

3a   3b
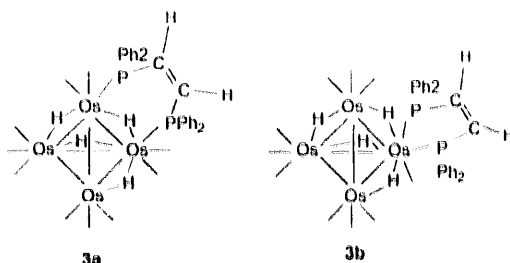
1. Introduction

There has been considerable interest in the study of the tetraosmium hydride carbonyl cluster $[Os_4(\mu\text{-H})_4(CO)_{12}]$ [1]. It has been shown that $[Os_4(\mu\text{-H})_4(CO)_{12}]$ reacted with alkenes to give alkene-substituted tetraosmium clusters in good yields [2]. However, the CO substitution reaction by other nucleophiles occurred much more readily with the activated tetraosmium cluster $[Os_4(\mu\text{-H})_4(CO)_{10}(NCMe)_2]$ 1. For example, reaction of 1 with cyclohexa-1,3-diene gave a range of products including cyclohexenyl, cyclohexadiene and benzene containing clusters [3,4]. Furthermore, 1 has been used as a catalyst in the cycloligomerization of trimethylene sulfide to give polythioethers [5]. It has

also been reported that the related tetraruthenium cluster can be incorporated in a phosphine-functionalized polymer to give $[Ru_4(\mu\text{-H})_4(CO)_{12-x}(Ph_2P\text{-polymer})_x]$ [6] ($x = 1$, 3, and 4). Such polymer-immobilized clusters have been used to catalyse olefin hydrogenation. Although some triosmium carbonyl clusters containing phosphine ligands have also been incorporated in the polymer matrix for studies of their catalytic reaction [7,8], the immobilized tetraosmium clusters for a similar study have not been reported. To establish such a catalytic system, an understanding in the chemistry of the phosphine clusters $[Os_4(\mu\text{-H})_4(CO)_{10}(PR_3)_2]$ is important. Surprisingly, the structurally characterized phosphine-containing derivatives of $[Os_4(\mu\text{-H})_4(CO)_{12}]$ are very rare. The only example we are aware of is $[Os_4(\mu\text{-H})_4(CO)_{11}\{P(OMe)_3\}]$ [9]. We herein report the results of the reaction between $[Os_4(\mu\text{-H})_4(CO)_{10}(NCMe)_2]$ and a series of bidentate phosphine

* Corresponding author. Tel.: +852-28592157; fax: +852-25472933; e-mail: wtwong@hkucc.hku.hk.

ligands to produce some novel diphosphine-substituted tetraosmium hydrido clusters [Os$_4$(μ-H)$_4$(CO)$_{10}$L], (L = dppm, dppee, dppp or dppf). Among them, a notable observation is that the ligand bis(diphenylphosphino)ethylene (dppee) can either act as a bridging or chelating ligand.

2. Results and discussion

The activated tetraosmium hydrido cluster **1** was synthesized by the reaction of the tetraosmium carbonyl cluster [Os$_4$(μ-H)$_4$(CO)$_{12}$] with 2 equivalents of Me$_3$NO in MeCN. The reaction gave an orange solid of **1** in good yield. Details of the preparation have been previously reported, however, the structure of **1** is not available. Crystals of cluster **1** suitable for X-ray diffraction studies were obtained by slow diffusion of diethylether into a CH$_2$Cl$_2$ solution of the complex at room temperature for three days. The crystal structure of cluster **1** contains two crystallographically independent molecules within the asymmetric unit. A perspective view of one of the molecules is shown in Fig. 1. Some selected bond parameters are tabulated in Table 1.

Cluster **1**, like [Os$_4$(μ-H)$_4$(CO)$_{12}$], possesses a tetrahedral metal core. The carbonyl groups in cluster **1** are all terminally bonded to the osmium atoms, and the two acetonitrile ligands are coordinated to the same osmium atom. The molecule possesses approximate C_s symmetry. Interestingly, two MeCN ligands were previously believed to coordinate to different metal centres as in [Os$_3$(CO)$_{10}$(NCMe)$_2$] [10].
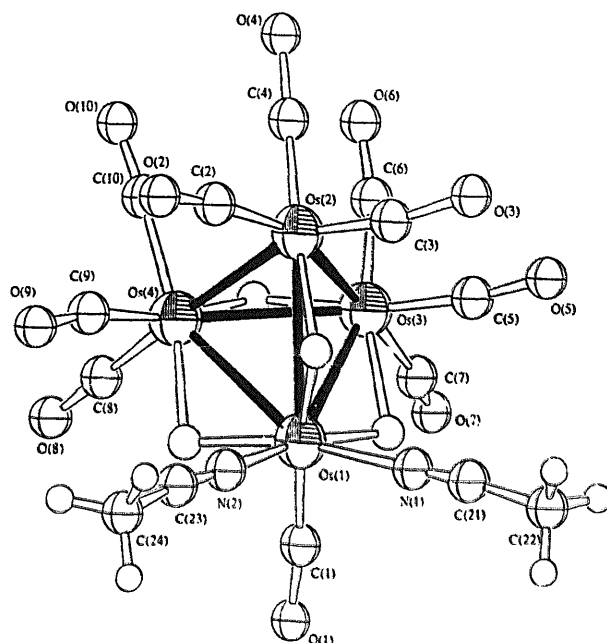

Fig. 1. An perspective drawing of [H$_4$Os$_4$(CO)$_{10}$(NCMe)$_2$] **1**.

2.1. Reaction of [Os$_4$(μ-H)$_4$(CO)$_{10}$(NCMe)$_2$] **1** with dppm and dppp

The reaction of a 3-fold excess of bis(diphenylphosphino)methane (dppm) or bis(diphenylphosphino)propane (dppp) with [Os$_4$(μ-H)$_4$(CO)$_{10}$(NCMe)$_2$] in refluxing CH$_2$Cl$_2$ gave the complexes [Os$_4$(μ-H)$_4$(CO)$_{10}$(μ-dppm)] **2** or [Os$_4$(μ-H)$_4$(CO)$_{10}$(μ-dppp)] **4**, as the major products respectively (Scheme 1). Single
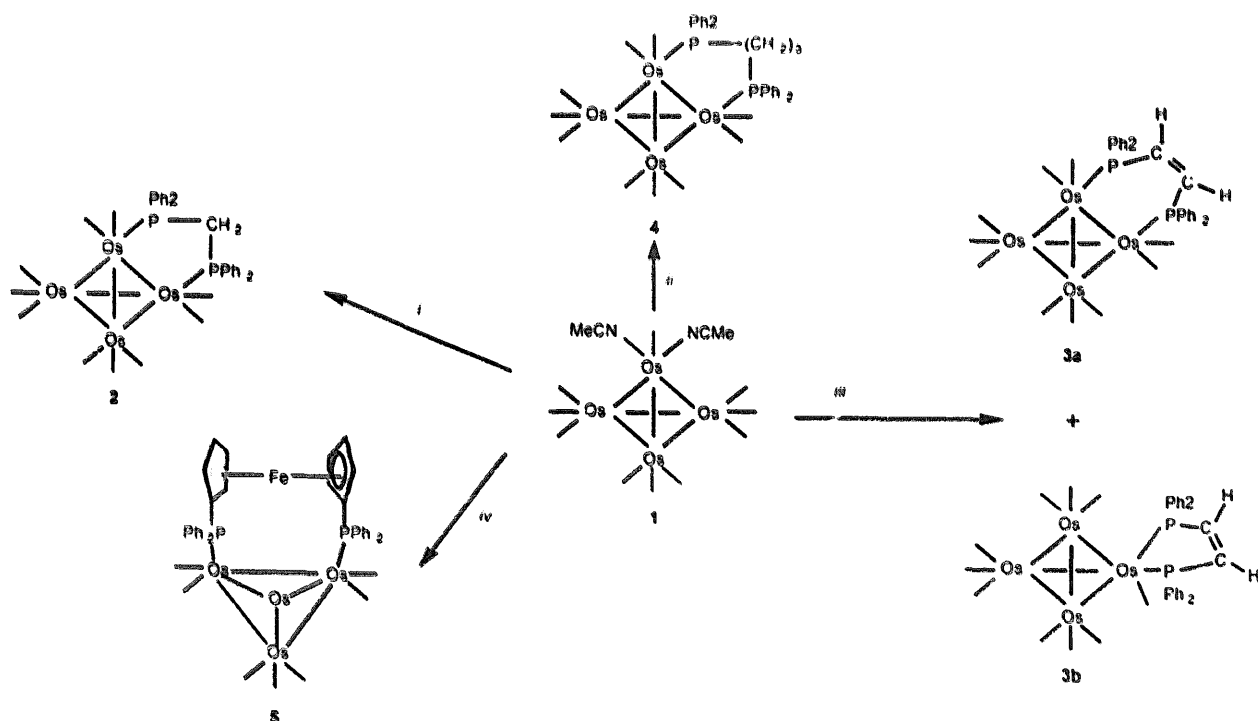
Scheme 1.

Table 1
Selected bond distances (Å) and angles (°) for cluster 1

Molecule 1		Molecule 2	
Os(1)–Os(2)	2.998(3)	Os(5)–Os(6)	2.919(3)
Os(1)–Os(3)	2.935(3)	Os(5)–Os(7)	2.991(3)
Os(1)–Os(4)	2.915(3)	Os(5)–Os(8)	2.931(3)
Os(2)–Os(3)	2.810(3)	Os(6)–Os(7)	2.816(3)
Os(2)–Os(4)	2.810(3)	Os(6)–Os(8)	2.931(3)
Os(3)–Os(4)	2.930(3)	Os(7)–Os(8)	2.805(3)
Os(1)–N(1)	2.07(5)	Os(5)–N(3)	1.94(5)
Os(1)–N(2)	2.02(4)	Os(5)–N(4)	2.04(4)
N(1)–C(21)	1.07(7)	N(3)–C(25)	1.18(7)
N(2)–C(23)	1.14(6)	N(4)–C(27)	1.15(6)
N(1)–Os(1)–N(2)	89(1)	N(3)–Os(5)–N(4)	93(1)
Os(2)–Os(1)–Os(3)	56.53(7)	Os(6)–Os(5)–Os(7)	56.89(7)
Os(2)–Os(1)–Os(4)	56.76(8)	Os(6)–Os(5)–Os(8)	60.13(7)
Os(3)–Os(1)–Os(4)	60.10(7)	Os(7)–Os(5)–Os(8)	56.52(7)
Os(1)–Os(2)–Os(3)	60.60(8)	Os(5)–Os(6)–Os(7)	62.84(7)
Os(1)–Os(2)–Os(4)	60.14(8)	Os(5)–Os(6)–Os(8)	60.13(7)
Os(3)–Os(2)–Os(4)	62.82(8)	Os(7)–Os(6)–Os(8)	58.38(8)
Os(1)–Os(3)–Os(2)	62.87(7)	Os(5)–Os(7)–Os(6)	60.27(7)
Os(1)–Os(3)–Os(4)	59.62(7)	Os(5)–Os(7)–Os(8)	60.66(8)
Os(2)–Os(3)–Os(4)	58.61(8)	Os(6)–Os(7)–Os(8)	62.86(8)
Os(1)–Os(4)–Os(2)	63.10(7)	Os(5)–Os(8)–Os(6)	59.74(7)
Os(1)–Os(4)–Os(3)	60.27(7)	Os(5)–Os(8)–Os(7)	62.82(7)
Os(2)–Os(4)–Os(3)	58.57(8)	Os(6)–Os(8)–Os(7)	58.76(7)
N(1)–C(21)–C(22)	171(7)	N(3)–N(25)–C(26)	165(6)
N(2)–C(23)–C(24)	165(6)	N(4)–C(27)–C(28)	174(5)

crystals of **2** and **4** for X-ray diffraction analyses were obtained by a dichloromethane/*n*-hexane layering procedure at room temperature. The molecular structures of clusters **2** and **4** with atom numbering schemes are depicted in Figs. 2 and 3, respectively, and selected bond distances and angles are shown in Tables 2 and 3.
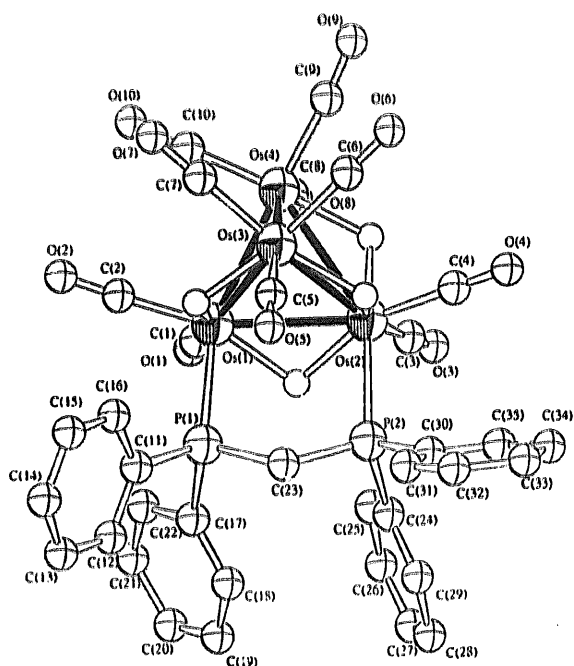

Fig. 2. An perspective drawing of [H₄Os₄(CO)₁₀(μ-dppm)] **2**.
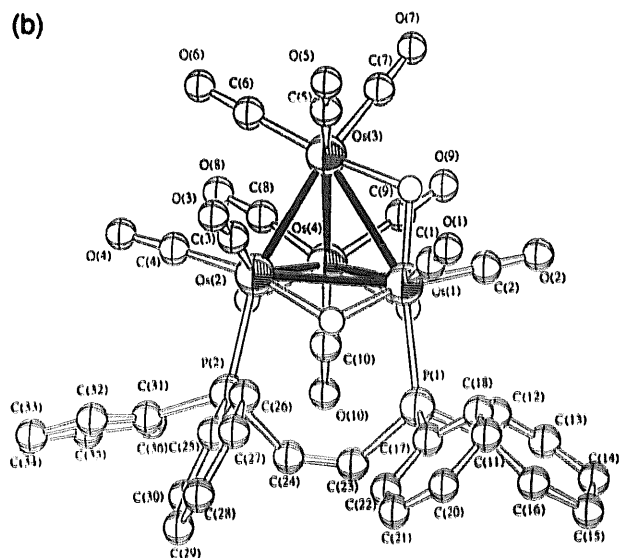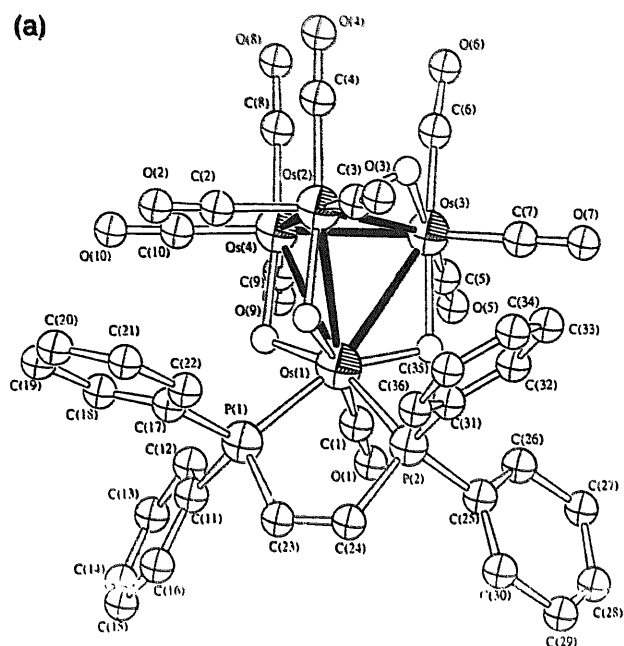
Fig. 3. An perspective drawing of [H₄Os₄(CO)₁₀(μ-dppp)] **4**. An perspective drawing of [H₄Os₄(CO)₁₀(μ-dppee)] **3a**.

Table 2
Selected bond distance (Å) and angles (°) for cluster 2

Os(1)–Os(2)	2.980(1)	Os(1)–Os(3)	2.965(1)
Os(1)–Os(4)	2.786(2)	Os(1)–P(1)	2.339(5)
Os(2)–Os(3)	2.972(1)	Os(2)–Os(4)	2.954(1)
Os(2)–P(2)	2.354(5)	Os(3)–Os(4)	2.806(1)
Os(2)–Os(1)–Os(3)	59.98(3)	Os(2)–Os(1)–Os(4)	61.52(3)
Os(2)–Os(1)–P(1)	94.5(1)	Os(3)–Os(1)–Os(4)	58.30(3)
Os(1)–Os(2)–Os(3)	59.76(3)	Os(1)–Os(2)–Os(4)	56.00(3)
Os(1)–Os(2)–P(2)	90.5(1)	Os(3)–Os(2)–Os(4)	56.52(3)
Os(1)–Os(3)–Os(2)	60.26(3)	Os(1)–Os(3)–Os(4)	57.65(3)
Os(2)–Os(3)–Os(4)	61.41(3)	Os(1)–Os(4)–Os(2)	62.48(3)
Os(1)–Os(4)–Os(3)	64.05(3)	Os(2)–Os(4)–Os(3)	62.07(3)

Table 3
Selected bond distances (Å) and angles (°) for cluster 4

Os(1)–Os(2)	2.996(2)	Os(1)–Os(3)	2.806(2)
Os(1)–Os(4)	2.953(2)	Os(1)–P(1)	2.350(7)
Os(2)–Os(3)	2.961(2)	Os(2)–Os(4)	2.996(2)
Os(2)–P(2)	2.353(7)	Os(3)–Os(4)	2.807(2)
Os(2)–Os(1)–Os(3)	61.27(4)	Os(2)–Os(1)–Os(4)	60.47(4)
Os(2)–Os(1)–P(1)	112.8(2)	Os(3)–Os(1)–Os(4)	58.27(4)
Os(1)–Os(2)–Os(3)	56.20(4)	Os(1)–Os(2)–Os(4)	59.05(4)
Os(1)–Os(2)–P(2)	105.4(2)	Os(3)–Os(2)–Os(4)	56.22(4)
Os(1)–Os(3)–Os(2)	62.53(4)	Os(1)–Os(3)–Os(4)	63.49(5)
Os(2)–Os(3)–Os(4)	62.52(4)	Os(1)–Os(4)–Os(2)	60.47(4)
Os(1)–Os(4)–Os(3)	58.24(4)	Os(2)–Os(4)–Os(3)	61.27(4)

respectively. The molecular structures of clusters 2 and 4 each shows a distorted tetrahedral tetraosmium metal core which is coordinated with a bridging bidentate phosphine ligand. For 2, the Os(1)–Os(4) and Os(3)–Os(4) bonds [2.786(2) Å, 2.806(1) Å] are shorter than the mean of the other four Os–Os bond distances [2.968(9)] in cluster 2. This is probably due to the absence of bridging hydride; the same observation was also made in the Os(1)–Os(3) and Os(3)–Os(4) bonds of cluster 4. The Os(1)–P(1)–C(23)–P(2)–Os(2) ring in cluster 2 adopts a twisted five membered ring conformation with C(23) lying above the ring. The seven-mem-

bered ring [Os(1)–P(1)–C(23)–C(24)–C(25)–P(2)–Os(2)] in cluster 4 is also twisted which can be attributed to the large torsional strain of the ring.

The two compounds have been characterized by conventional solution spectroscopic methods. The spectroscopic data are summarized in Table 4. Their positive FAB mass spectra both exhibit an envelope with a molecular ion peak at 1430 (2) and 1458 (4), respectively. The ^{1}H NMR spectrum of cluster 2 shows a double doublet at δ 2.73 which is attributable to the CH_2 protons. The signals at δ −19.43 and −18.80 of equal intensity are due to the bridging hydrides in the metal core. Cluster 4 shows three multiplets at δ 2.17, 2.67 and 2.75 from the three CH_2 protons in the alkyl chain, where the two multiplets at δ −19.73 and −20.08 are due to the four hydrides on the metal core. The ^{31}P NMR spectrum shows signals at δ −21.91, −29.63 for 2 and δ −17.72, −6.05 for 4, which are attributable to the coordination of phosphine to the cluster metal core. However, the solid state structures of both 2 and 4 are not consistent with their ^{1}H NMR spectroscopic data. Although it is likely that the clusters 2 and 4 will undergo fluxional processes, we cannot work out any structure that is compatible with all the solution NMR data without proposing two hydride atoms bridging the same Os–Os edge.

Table 4
Summary of spectroscopic data of cluster 2–5

Compound	IR (ν_{CO})[a] (cm^{-1})	^{1}H NMR[b] (δ, J(Hz))	^{31}P NMR[c] (δ, J(Hz))	MS[d]
2	2074s, 2051s, 2031vs, 2006s, 1983m, 1955w	−19.43 (m, 2H, OsH) −18.80 (m, 2H, OsH) 2.73 (dd, 2H, J(PH) = 2 Hz, CH$_2$) 7.52 (m, 20H, 4C$_6$H$_5$)	−21.91 (s, PPh$_2$Os) −29.63 (s, PPh$_2$Os)	1430 (1430)
3a	2073s, 2048s, 2029vs, 2002s, 1965m, 1944w	−19.06 (m, 4H, OsH) 3.51 (m, 2H, CH=CH) 7.37 (m, 20H, C$_6$H$_5$)	−26.81 (broad, PPh$_2$Os)	1441 (1442)
3b	2079s, 2050s, 2019s, 2000s, 1975m, 1942w	−22.34 (s, 1H, OsH) −18.99 (s, 1H, OsH) −17.54 (s, 1H, OsH) −17.02 (s, 1H, OsH) 3.50 (m, 2H, CH=CH) 7.64 (m, 20H, C$_6$H$_5$)	34.25 (s, PPh$_2$Os) 41.14 (s, PPh$_2$Os)	1441 (1442)
4	2072s, 2048s, 2029vs, 2002s, 1987m, 1956w	−19.73 (m, 2H, OsH) −20.08 (m, 2H, OsH) 2.17 (m, 2H, CH$_2$) 2.67 (m, 2H, CH$_2$) 2.75 (m, 2H, CH$_2$) 7.31–7.60 (m, 20H, C$_6$H$_5$)	−17.72 (s, PPh$_2$Os) −6.05 (s, PPh$_2$Os)	1458 (1458)
5	2073s, 2048s, 2029vs, 2004s, 1989m, 1960m	−18.67 (m, 2H, OsH) −19.05 (m, 2H, OsH) 4.06 (m, 2H C$_5$H$_4$) 4.26 (d, 4H, J(PH) = 14Hz), C$_5$H$_4$) 4.48 (s, 2H, C$_5$H$_4$) 7.46 (m, 20H, C$_6$H$_5$)	−16.70 (s, PPh$_2$Os)	1599 (1600)

[a] In CH$_2$Cl$_2$.
[b] In CD$_2$Cl$_2$.
[c] In CDCl$_3$.
[d] Calculated values in parentheses.
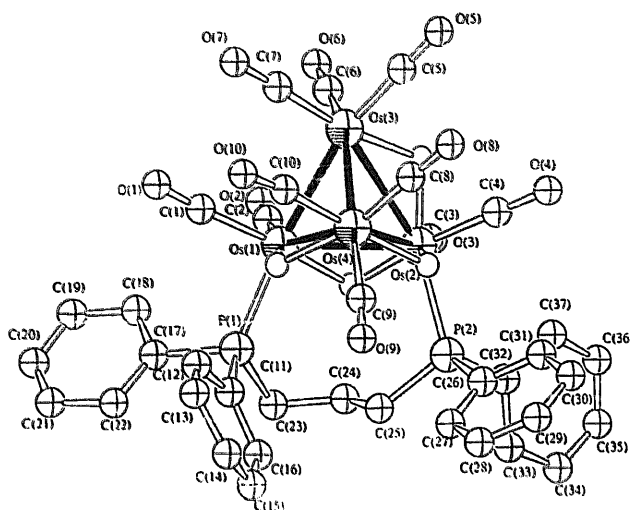
Fig. 4. An perspective drawing of [H$_4$Os$_4$(CO)$_{10}$(η^2-dppee)] 3b.

2.2. Reaction of [Os$_4$(μ-H)$_4$(CO)$_{10}$(NCMe)$_2$] 1 with dppee

A four-fold excess of bis(diphenylphosphino)ethylene (dppee) was allowed to react with cluster 1 in refluxing CH$_2$Cl$_2$ to give two isomeric clusters 3a and 3b with the stoichiometry [Os$_4$(μ-H)$_4$(CO)$_{10}$(dppee)]. Bis(diphenylphosphino)ethylene adopts a bridging mode in 3a but it acts as a chelating ligand in the formation of 3b. The dppee-bridged cluster 3a shows a broad multiplet at δ −19.06 in the ^{1}H NMR spectrum. This is assigned to the four hydrides in the tetraosmium core, while the corresponding four hydrides in the dppee-chelated cluster 3b appeared as four singlets at δ −22.34, −18.99, −17.54 and −17.02. The positive FAB mass spectra of both 3a and 3b show a parent ion envelope centred at m/z 1441, indicating they have the same molecular mass and are probably isomeric to each other. Their IR spectra show a similar carbonyl absorp-
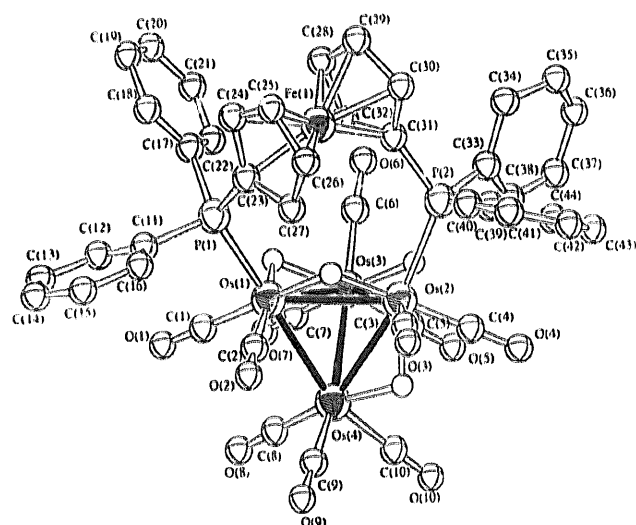

Fig. 5. An perspective drawing of [H$_4$Os$_4$(CO)$_{10}$(μ-dppf)] 5.

tion pattern in the range of 2080–1940 cm^{-1}. However, the ^{31}P NMR spectrum of cluster 3a showed a broad multiplet at δ −26.81, whereas the phosphorus in 3b gave signals at δ 34.25 and 41.14. The downfield shift of the phosphorus atoms in cluster 3b is probably due to the chelating effect of the bidentate phosphine ligand. Previous studies have shown that a phosphorus atom involved in a five membered chelated ring experiences anomalously large nuclear deshielding upon coordination [11,12]. Orange crystals of cluster 3a and yellow crystals of 3b suitable for X-ray diffraction analyses were obtained by slow evaporation of the respective solutions of cluster 3a and 3b in CH$_2$Cl$_2$/n-hexane. The molecular structures of clusters 3a and 3b are shown in Figs. 4 and 5, respectively. The selected bond parameters are given in Tables 5 and 6, respectively.

The molecular structure of cluster 3a is very similar to that of cluster 2 in which a bidentate phosphine ligand bridges across Os(1) and Os(2). The Os(2)–Os(3) [2.782(1)Å] and Os(3)–Os(4) [2.804(1) Å] bonds in cluster 3a are shorter than the average of the other four bond lengths in cluster 3a [average 2.96(2) Å]. Again this may be attributed to the presence of the bridging hydrides along the longer Os–Os bonds. In cluster 3a, the six membered rings [Os(1)–P(1)–C(23)–C(24)–P(2)–Os(2)] forms a twisted boat conformation. The bidentate phosphine ligand in cluster 3b is no longer bridging to the two osmium atoms, but chelates one

Table 5
Selected bond distances (Å) and angles (°) for cluster 3a

Os(1)–Os(2)	2.985(1)	Os(1)–Os(3)	2.964(1)
Os(1)–Os(4)	2.970(1)	Os(1)–P(1)	2.358(6)
Os(2)–Os(3)	2.782(1)	Os(2)–Os(4)	2.930(1)
Os(2)–P(2)	2.324(6)	Os(3)–Os(4)	2.804(1)
Os(2)–Os(1)–Os(3)	55.77(3)	Os(2)–Os(1)–Os(4)	58.95(3)
Os(2)–Os(1)–P(1)	99.3(2)	Os(3)–Os(1)–Os(4)	56.40(3)
Os(1)–Os(2)–Os(3)	61.73(3)	Os(1)–Os(2)–Os(4)	60.27(3)
Os(1)–Os(2)–P(2)	101.1(1)	Os(3)–Os(2)–Os(4)	58.72(3)
Os(1)–Os(3)–Os(2)	62.50(3)	Os(1)–Os(3)–Os(4)	61.91(3)
Os(2)–Os(3)–Os(4)	63.27(3)	Os(1)–Os(4)–Os(2)	60.78(3)
Os(1)–Os(4)–Os(3)	61.69(3)	Os(2)–Os(4)–Os(3)	58.00(3)

Table 6
Selected bond distances (Å) and angles (°) for cluster 3b

Os(1)–Os(2)	3.0256(9)	Os(1)–Os(3)	2.9659(9)
Os(1)–Os(4)	2.9614(9)	Os(1)–P(1)	2.300(4)
Os(2)–Os(3)	2.9331(9)	Os(2)–Os(4)	2.8132(9)
Os(1)–P(2)	2.313(4)	Os(3)–Os(4)	2.821(1)
Os(2)–Os(1)–Os(3)	58.61(2)	Os(2)–Os(1)–Os(4)	56.04(2)
Os(2)–Os(1)–P(1)	108.7(1)	Os(3)–Os(1)–Os(4)	56.84(2)
Os(1)–Os(2)–Os(3)	59.68(2)	Os(1)–Os(2)–Os(4)	60.83(2)
Os(2)–Os(1)–P(2)	110.8(1)	Os(3)–Os(2)–Os(4)	58.76(2)
Os(1)–Os(3)–Os(2)	61.71(2)	Os(1)–Os(3)–Os(4)	61.50(2)
Os(2)–Os(3)–Os(4)	58.50(2)	Os(1)–Os(4)–Os(2)	63.13(2)
Os(1)–Os(4)–Os(3)	61.66(2)	Os(2)–Os(4)–Os(3)	62.74(2)
P(1)–Os(1)–P(2)	84.5(2)		

osmium atom Os(1). The diphosphine ligand and the Os(1) atom form a five-membered ring structure, with the angle P(1)–Os(1)–P(2) being 84.5°. The mean of the other four Os–Os bond lengths [2.97(3) Å] in cluster 3b is longer than the Os(2)–Os(4) and Os(3)–Os(4) bonds [2.8132(9) Å and 2.821(1) Å]. Again, this is presumably due to the bridging hydrides in other Os–Os bonds.

The conformations of both clusters 3a and 3b have been studied by molecular mechanical calculations using MM2 parameters. The optimization of the structures of clusters 3a and 3b was carried out until convergence had been reached. The result of optimization shows that the total energy of cluster 3a is larger than that of cluster 3b. Since the yield of cluster 3a is much larger than that of cluster 3b, this indicates that cluster 3a is probably kinetically favourable whereas cluster 3b is thermodynamically favoured. The result agrees well with the ring strain of the two clusters, in which the five membered ring possesses a smaller ring strain than that of the six membered ring. However, the interconvertion of 3a and 3b is not observed at room temperature or even in refluxing CH_2Cl_2.

2.3. Reaction of $[Os_4(\mu\text{-}H)_4(CO)_{10}(NCMe)_2]$ 1 with dppf

When cluster 1 is reacted with a two-fold excess of 1,1'-bis(diphenylphosphino)ferrocene in CH_2Cl_2 for 6 h, a new cluster $[Os_4(\mu\text{-}H)_4(CO)_{10}(\mu\text{-dppf})]$ 5 is isolated as a major orange product. The IR absorption pattern of the CO stretching activity of cluster 5 is very similar to those of clusters 2–4. The ferrocenyl ligand gives three signals in the ^1H NMR at δ 4.06, 4.26 and 4.48 corresponding to the eight protons in the ferrocenyl moiety. The ^{31}P NMR spectrum of cluster 5 gives a singlet at $\delta = 16.70$ due to the coordinated P moieties. The positive FAB mass spectrum of cluster 5 shows an envelope of parent ion peak centred at m/z 1599. Single orange crystals of cluster 5 were obtained by slow evaporation of 5 in CH_2Cl_2/n-hexane solution. The molecular structure of cluster 5 is depicted in Fig. 6 and selected bond parameters are tabulated in Table 7.

The molecular structure of cluster 5 consists of an Os_4 tetrahedron with the dppf ligand bridging across an Os–Os edge via two P atoms. The Os(1)–Os(4) and Os(3)–Os(4) edges [2.7989(7) and 2.8088(5), respectively] are found to be shorter than the other four Os–Os bond distances due to the absence of bridging hydrides as previously mentioned. The angle at the phosphine bound osmium atom in cluster 5 is the largest among clusters 2–5. The Os(2)–Os(1)–P(1) and Os(1)–Os(2)–P(2) fragments have an angle of 118.08 and 114.09 respectively. Since the ferrocene group in cluster 5 is much larger and less flexible than the alkane or

Table 7
Selected bond distances (Å) and angles (°) for cluster 5

Os(1)–Os(2)	2.9982(7)	Os(1)–Os(3)	2.9593(8)
Os(1)–Os(4)	2.7989(7)	Os(1)–P(1)	2.349(4)
Os(2)–Os(3)	2.9854(5)	Os(2)–Os(4)	2.9801(5)
Os(2)–P(2)	2.356(2)	Os(3)–Os(4)	2.8088(5)
Os(2)–Os(1)–Os(3)	60.14(2)	Os(2)–Os(1)–Os(4)	61.76(2)
Os(2)–Os(1)–P(1)	118.08(6)	Os(3)–Os(1)–Os(4)	58.31(2)
Os(1)–Os(2)–Os(3)	59.28(2)	Os(1)–Os(2)–Os(4)	55.83(2)
Os(1)–Os(2)–P(2)	114.90(9)	Os(3)–Os(2)–Os(4)	56.18(1)
Os(1)–Os(3)–Os(2)	60.57(2)	Os(1)–Os(3)–Os(4)	57.98(2)
Os(2)–Os(3)–Os(4)	61.82(1)	Os(1)–Os(4)–Os(2)	62.42(2)
Os(1)–Os(4)–Os(3)	63.71(2)	Os(2)–Os(4)–Os(3)	62.01(1)

alkylene chains in 2–4, it is reasonable for cluster 5 to show larger angles.

3. Experimental

None of the compounds reported here are particularly air-sensitive. However, all reactions and manipulations were carried out under Ar with the use of standard inert-atmosphere and Schlenk techniques. The reactions were monitored by solution IR spectroscopy in the carbonyl stretching region. Solvents were dried by standard procedures [13] and freshly distilled prior to use. The ^1H NMR spectra were recorded on a Bruker DPX 300 NMR spectrometer. The ^{31}P NMR spectra were recorded on a Bruker DPX 500 NMR spectrometer (85% H_3PO_4 for ^{31}P). Mass spectra were obtained on a Finnigan MAT 95 instrument with fast atom bombardment technique.

All chemicals, except where stated, were purchased from commercial sources and used as received without any further purification. The starting cluster $[H_4Os_4(CO)_{10}(NCMe)_2]$ was prepared from $[H_4Os_4(CO)_{12}]$ following the literature [14,15]. Routine separation of products was performed in air by thin-layer chromatography using plates coated with Merck Kieselgel 60 GF$_{254}$.

3.1. Preparation of $[H_4Os_4(CO)_{10}(\mu\text{-dppm})]$ 2 and $[H_4Os_4(CO)_{10}(\mu\text{-dppp})]$ 4

The cluster 1 (113mg, 0.1mmol) and a 4-fold excess of bis(diphenylphosphino)methane (153mg, 0.4mmol) or 1,4-bis(diphenylphosphino)propane (171mg, 0.4mmol) in CH_2Cl_2 (25cm³) were heated to reflux under an argon atmosphere for 4 h until all starting materials had been consumed as monitored by TLC. The solvent was removed under reduced pressure and the residue was chromatographed on silica plate with n-hexane/dichloromethane (7:3, v/v) as eluent. Cluster 2 was isolated as a deep yellow solid $[H_4Os_4(CO)_{10}(\mu\text{-dppm})]$ ($R_f = 0.6$) in 45% yield (65

Table 8
Crystallographic data, data collection and structure solution parameters for cluster 1–5

	1	2	3a	3b	4	5
Empirical formula	$Os_4C_{14}O_{10}N_2H_{10}$	$Os_4P_2O_{10.50}C_{37}H_{37}$	$Os_4P_2C_{36}O_{10}H_{28}$	$Os_4P_2C_{37}O_{10}H_{28}Cl_2$	$Os_4O_{10}P_2C_{37}H_{30}$	$Os_4FeP_2O_{10}C_{44}H_{32}$
M	1127.04	1466.39	1443.36	1526.28	1457.39	1599.33
Crystal color, habit	Yellow	Yellow	Orange	Orange	Yellow	Orange
Crystal size/mm	$0.18 \times 0.20 \times 0.33$	$0.12 \times 0.17 \times 0.37$	$0.28 \times 0.29 \times 0.33$	$0.18 \times 0.18 \times 0.38$	$0.12 \times 0.34 \times 0.36$	$0.2 \times 0.2 \times 0.28$
Crystal system	Monoclinic	Triclinic	Monoclinic	Monoclinic	Monoclinic	Orthorhombic
Space group	$P2_1$ (No. 4)	$P\bar{1}$ (No. 2)	$P2_1/n$ (No. 14)	$P2_1/c$ (No. 14)	$P2_1/c$ (No. 14)	Pbca (No. 61)
$a/\text{Å}$	12.416(1)	11.401(4)	12.920(1)	11.685(1)	9.315(1)	21.828(1)
$b/\text{Å}$	14.917(1)	18.654(4)	19.915(1)	18.402(1)	20.933(1)	17.318(1)
$c/\text{Å}$	12.575(1)	10.297(5)	15.597(1)	20.369(2)	21.289(2)	24.135(2)
$\alpha/°$	90	92.00(3)	90	90	90	90
$\beta/°$	91.54(2)	109.97(3)	102.43(2)	102.54(2)	98.94(2)	90
$\gamma/°$	90	87.98(2)	90	90	90	90
$U/\text{Å}^3$	2328.2(2)	2056(1)	3919.1(5)	4275.4(7)	4100.7(6)	9123.4(9)
Z	4	2	4	4	4	8
$D_c/\text{g cm}^{-3}$	3.215	2.368	2.446	2.371	2.360	2.329
$F(000)$	1968	1342	2632	2792	2664	5888
$\mu(\text{Mo-K}_\alpha)/\text{cm}^{-1}$	217.95	142.42	130.54	120.94	124.77	115.29
Diffractometer	MAR-research image plate scanner	AFC7R	MAR-research image plate scanner	MAR-research image plate scanner	MAR-research image plate scanner	MAR-research image plate scanner
2θ Range collect/°	51.4	45.0	51.1	51.1	51.2	51.3
No. reflections collected	20566	5706	23919	28453	29348	30856
No. unique reflections	4372	5376	7499	7845	7705	7888
R_{int}	0.067	0.049	0.055	0.063	0.095	0.062
No. observed reflections $[I > 3\sigma(I)]$	2739	3840	3208	3125	2393	4661
No. of variables	0	235	239	251	293	280
R [a]	0.051	0.043	0.052	0.040	0.042	0.034
R' [b]	0.065	0.051	0.067	0.046	0.074	0.027
Goodness to fit	1.94	2.12	1.96	2.20	2.97	1.83
Residual electron density $(e\text{Å}^3)$	2.38 to −2.43	1.49 to −1.67	1.40 to −3.27	1.48 to −1.91	2.59 to −1.73	0.92 to −1.04

[a] $R = \Sigma\|F_o| - |F_c\|/|F_o|$.
[b] $R' = [\Sigma\omega(|F_o| - |F_c|)^2/\Sigma\omega F_0^2]^{1/2}$.

mg) (Found: C, 29.35; H, 1.88; P, 4.19%. Calc. for $Os_4C_{35}H_{26}P_2O_{10}$: C, 29.25; H, 1.82; P, 4.31%), and cluster **4** was isolated as a pale yellow solid $[H_4Os_4(CO)_{10}(\mu\text{-dppp})]$ ($R_f = 0.5$) in 30% yield (44 mg) (Found: C, 30.68; H, 1.84; P, 4.12%. Calc. for $Os_4C_{37}H_{30}P_2O_{10}$: C, 30.49; H, 2.07; P, 4.25%).

3.2. Preparation of $[H_4Os_4(CO)_{10}(\mu\text{-dppee})]$ 3a and $[H_4Os_4(CO)_{10}(\eta^2\text{-dppee})]$ 3b

The cluster **1** (1.13 mg, 0.1 mmol) and a 4-fold excess of cis-bis(diphenylphosphino)ethylene (158 mg, 0.4 mmol) were heated to reflux in dichloromethane (25 cm³) under an argon atmosphere for 3 h. The solvent was evaporated to dryness under vacuum. The residue was purified by TLC using n-hexane dichloromethane (7:3, v/v) as eluent. Two bands were obtained. The orange solid was characterized as cluster **3a** ($R_f = 0.6$) in 50% yield (72 mg) (Found: C, 30.17; H, 1.93; P, 4.25%. Calc. for $Os_4C_{36}H_{26}P_2O_{10}$: C, 30.00; H, 1.82;P, 4.30%) and the yellow product was $[H_4Os_4(CO)_{10}(\eta^2\text{-dppee})]$ **3b** ($R_f = 0.55$) in 10% yield (14 mg) (Found: C, 30.21; H, 1.89%. Calc. for $Os_4C_{36}H_{26}P_2O_{10}$: C, 30.00; H, 1.82; P, 4.30%).

3.3. Preparation of $[H_4Os_4(CO)_{10}(\mu\text{-dppf})]$ 5

The cluster **1** (113 mg, 0.1 mmol) and a 2-fold excess of 1,1'-bis(diphenylphosphino)ferrocene (110 mg, 0.2 mmol) were stirred in dichloromethane (25 cm³) for 6 h under an argon atmosphere. The solvent was removed under reduced pressure. The residue was purified by TLC using n-hexane dichloromethane (8:2, v/v) as eluent. An intense yellow product of cluster **5** was isolated ($R_f = 0.4$) in 30% yield (47mg) (Found: C, 33.13; H, 2.21; P, 3.65. Calc. for $Os_4FeP_2C_{44}H_{32}O_{10}$: C, 33.04; H, 2.02; P, 3.87%).

3.4. Molecular modelling

Molecular modelling was carried out on a CAChe Tektronix computer. The parameters are: relaxation factor = 1, convergence to 0.004 kJ/mol, and the energy terms included: bond angles and stretch, dihedral angles and improper torsions, intramolecular van der Waals, electrostatic and hydrogen bond interactions.

Conformation of **3a** and **3b** were simulated and the predicted conformational energy of **3a** is 970.8 kJ/mol, while **3b** is 948.7 kJ/mol. The predicted average total energy for **3a** and **3b** are 8292.2 kJ/mol and 7837.9 kJ/mol, respectively. They are in agreement with the suggestion that **3a** is the kinetic product, while **3b** is the thermodynamic product.

4. X-ray crystallography

All pertinent crystallographic data and other experimental details are summarized in Table 8. Intensity data were collected at ambient temperature on either a MAR research image plate scanner (cluster **1**, **3a**, **3b**, **4** and **5**) or a Rigaku AFC7R diffractometer (**2**) using Mo-K_α radiation ($\lambda = 0.71073$ Å) with a graphite-crystal monochromator. For cluster studied by image plate scanner, 65 3° frames with an exposure time of 5 min. to 10 min. per frame were used to collect the intensity data. The $\omega - 2\theta$ scan technique with scan rate of 16 °min^{-1} (in ω) was using for cluster **2**. The intensity data were corrected for Lorentz and polarization effect. The ψ-scan method [16] was used for absorption correction for **2**. However, no absorption correction was made for other clusters. The structures were solved by a combination of direct methods (SIR88) [17] and difference Fourier techniques. The solutions were refined on F by full-matrix least-squares analysis with Os and P varied anisotropically until convergence was reached. The hydrogen atoms of the organic moieties were generated in their ideal positions (C–H 0.95 Å), while hydride atom positions were estimated by potential energy minimizations [18]. All the hydrogen atoms were included in the structure factors calculations but were not refined. For cluster **1**, attempts have been made to establish the polarity of the structure as it crystallized in a polar space group. However, the quantity of the data does not allow a conclusive distinct between two forms to be made. All calculations were performed on a Silica Graphics workstation using the program package TeXsan [19]. Addition materials available from the Cambridge Crystallographic Data Centre Comprise atomic coordinates, thermal displacement parameters and remaining bond distance and angles.

Acknowledgements

References

[1] R.K. Pomeroy, Tetranuclear clusters of ruthenium and osmium, in: D.F. Shriver, M.I. Bruce (Eds.), Comprehensive Organometallic Chemistry II, vol. 7, ch. 15, Elsevier Science B.V., Amsterdam, 1995.

[2] B.F.G. Johnson, J.W. Kelland, J. Lewis, S. Rehani, J. Organomet. 13 (1976) C42.

[3] H. Chen, B.F.G. Johnson, J. Lewis, D. Braga, F. Grepioni, E. Parisini, J. Chem. Soc., Dalton Trans. (1991) 215.

[4] B.F.G. Johnson, C.M. Martin, A.J. Blake, D. Reed, D. Braga, F. Grepioni, J. Chem. Soc., Dalton Trans. (1996) 2165.

[5] R.D. Adams, S.B. Falloon, Organometallics 14 (1995) 4594.

[6] Z. Otero-Schipper, J. Lieto, B.C. Gates, J. Catal. 63 (1980) 175.

[7] M.B. Freeman, M.A. Patrick, B.C. Gates, J. Catal. 73 (1982) 82.

[8] M. Wolf, J. Lieto, B.A. Matrana, D.B. Arnold, B.C. Gates, H. Knözinger, J. Catal. 89 (1984) 100.

[9] C.Y. Weil, L. Garlashelli, R. Bau, J. Organomet. Chem. 213 (1981) 63.

[10] P.A. Dawson, B.F.G. Johnson, J. Lewis, J. Puga, P.R. Raithby, M.J. Rosales, J. Chem. Soc., Dalton Trans. (1982) 233.

[11] S.O. Grim, W.L. Briggs, R.C. Barth, C.A. Tolman, J.P. Jesson, Inorg. Chem. 13 (1974) 1095.

[12] P.E. Garrou, Inorg. Chem. 14 (1975) 1435.

[13] D.D. Perrin, W.L.F. Armarego, D.R. Perrin, Purification of Laboratory Chemicals, 2nd ed., Pergamon, Oxford, 1980.

[14] H.d. Kaesz, S.A.R. Knox, J.W. Koepke, R.B. Saillant, J. Chem. Soc., Chem. Commun. (1971) 477.

[15] C. Zuccaro, G. Pampaloni, F. Calderazzo, Inorg. Synth. 26 (1989) 169.

[16] A.C.T. North, D.C. Phillps, F.S. Mathens, Acta Crystallogr. A 24 (1968) 351.

[17] M.C. Burla, N. Camalli, G. Cascarano, C. Giacovazzo, G. Polidor, R. Spagna, P. Viterbo, SIR88, J. Appl. Cryst. 22 (1989) 389.

[18] A.G. Orpen, J. Chem Soc, Dalton Trans. (1980) 2509.

[19] TeXsan: Crystal Structure Analysis Package, Molecular Structure Corp., 1985 and 1992.